ASTRONOMY & ASTROPHYSICS
SUPPLEMENT SERIES

JANUARY 1987, PAGE 283

*Astron. Astrophys. Suppl. Ser.* **67**, 283-296 (1987)

# The final COS-B database : in-flight calibration of sensitivity and instrumental background behaviour

A. W. Strong ([4]), J. B. G. M. Bloemen ([1,*]), F. Lebrun ([5]), W. Hermsen ([1]), H. A. Mayer-Hasselwander ([4]) and R. Buccheri ([2,3])

The Caravane Collaboration for the COS-B satellite :

([1]) Laboratory for Space Research, Leiden, The Netherlands
([2]) Istituto di Fisica Cosmica del CNR, Milano, Italy
([3]) Istituto di Fisica Cosmica e Informatica del CNR, Palermo, Italy
([4]) Max-Planck Institut für Physik und Astrophysik, Institut für Extraterrestrische Physik, 8046 Garching-bei-München, F.R.G.
([5]) Service d'Astrophysique, Centre d'Etudes Nucléaires de Saclay, France
([6]) Space Science Department of the European Space Agency, ESTEC, Noordwijk, The Netherlands

*Received February 10, accepted April 8, 1986*

**Summary.** — This is one in a series of papers prepared in association with the release of the final COS-B database. Various aspects of the performance of the COS-B $\gamma$-ray telescope are studied using in-flight data. First, the time-variation of the sensitivity and background over the 6.7 years of the mission is investigated. COS-B observed many regions of the sky repeatedly over the mission lifetime, allowing the study of the temporal behaviour of the instrument. Using a multivariate optimization algorithm, the relative sensitivity for the 65 observation periods is determined to an accuracy generally better than 10 %. The temporal variations of the instrumental background, assumed to be related to a cosmic-ray scaler aboard the satellite, are simultaneously determined. Second, the dependence of the instrumental background on the inclination to the telescope axis is analysed using observations of high galactic latitude areas. The resulting corrections to the instrumental parameters are a necessary prerequisite for the combination of the data into large-scale maps for scientific analysis. The implementation of the corrections to give such maps is outlined.

**Key words :** COS-B — gamma rays — data analysis.

## 1. Introduction.

The ESA $\gamma$-ray satellite COS-B operated successfully from 1975 to 1982 providing observations of a large fraction of the sky in the 50-5000 MeV range. A detailed description of the final database (now publicly available) is given in Mayer-Hasselwander (1985) and Mayer-Hasselwander *et al.* (1986).

From the ground calibration phase of the project to the analysis of the flight data a large amount of information and experience relevant to the use and interpretation of the data has been acquired by the members of the Caravane Collaboration. Since this knowledge is essential to any future studies using the database, details of various aspects of the instrumental response of the COS-B telescope are being given in two papers. Mayer-Hasselwander *et al.* (1986) will include accelerator calibration of the energy response and sensitivity, and accelerator and in-flight determination of the angular resolution (point-spread function) ; the present paper describes in-flight calibration of sensitivity and background variations.

During the mission the instrumental response was generally quite stable, apart from occasional known instrumental malfunctions. The most important variation is the long-term fall-off in sensitivity, amounting to about 50 % by the end of the mission. In addition, changes in experimental configuration and variations due to the manual editing process led to additional fluctuations of sensitivity of typically 10 % and occasionally more. A long-term variation in the instrumental background also occurred. Since no direct in-flight calibration is possible, all such variations must be determined by comparison of observations of the same region of sky at different epochs. The observation program consisted of 65 pointings lasting typically one month each. Since the useful field of view has a radius of about 20° and most of the observations are concentrated in the galactic plane, the

(*) Present address : Dept. of Astronomy, University of California, Berkeley, CA 94720, U.S.A.
*Send offprint requests to :* A. W. Strong.

amount of overlap is large. This multiple coverage allows us to use the galactic disc emission as a stable « calibration source ».

## 2. Determination of temporal variations : general description.

Three types of temporal response variation can be distinguished :

(i) long term variations in sensitivity due to degradation in spark-chamber performance ;

(ii) shorter term period-to-period variations in effective sensitivity due to fluctuations in spark-chamber performance or to variations in the efficiency of the manual editing of the spark-chamber pictures.

(iii) long- and short-term variations in instrumental background arising from variations in the ambient cosmic-ray intensity induced by solar modulation.

A method of determination of the variations which uses a non-linear optimization technique has been successfully applied. The general principle is to use the Galactic emission as a stable « calibration source » to compare the response of the instrument at different epochs. The main problem is that observations far apart on the sky are effectively decoupled and in this case the method can give no information on the relative detector response ; however, the instrument pointing directions were fairly randomly distributed in time so that there should be no correlation between sensitivity and pointing direction, and this can be used as a strong constraint on the solution. The constraint is sufficient to allow complete solution of the problem without input of any additional information on the sensitivity variation ; an *a posteriori* check on the consistency of the results with known instrumental effects (malfunctions, etc.) can then be performed.

The method uses a statistic $\chi^2$ which compares each observation period with the predicted emission based on the summed periods. Minimizing $\chi^2$ gives the most consistent set of sensitivity values for the given data. The problem of decoupled periods mentioned above is addressed by adding a constraint which reduces the fluctuations in sensitivity to a specified level. A fluctuation parameter $S$ is defined which measures the r.m.s. deviation of the sensitivity from a simple long-term trend (represented by a constant followed by a linear falloff), and $\chi^2$ is minimized subject to a fixed value of $S$. In order not to bias the solution towards a particular long-term trend the parameters of the trend are left free. As $S$ is decreased the value of $\chi^2$ increases from its unconstrained value ; the actual choice of $S$ is not unique but a reasonable value can be derived from the fact that the fluctuations in sensitivity are typically around 10 %. The $S$ parameter also serves to show the accuracy of determination for the sensitivity estimate for a particular period : for some periods the values are strongly influenced by $S$ indicating that there is little information in the overlap with other periods, so that the value is pulled towards the average trend ; many periods on the other hand are hardly affected by $S$ since they are well determined by overlapping observations.

The variation in the background cannot in practice be determined for each period solely on the basis of overlapping observations because this involves too much freedom in the solution. Fortunately the variation is relatively small ($\sim 25$ % over 6 years) and it is correlated with the count rate in a scaler $(S_3)$ which is sensitive to the gross rate of cosmic-ray interactions in the instrument which are responsible for the background. In the present method the background change is assumed proportional to the change in the $S_3$ rate with the constant of proportionality for each energy range determined by minimizing $\chi^2$ for that range. In this way both long- and short-term background variations are included, at least to the extent that they are reflected in $S_3$ variations.

## 3. Determination of temporal variations : detailed description.

The gamma-ray sky (latitudes $|\, b \,| < 30°$) is divided into *subcells* of 1° square, and the field of view of each observation period (20° radius) is divided into *cells* of 100 square degrees by « raster » scans 1° wide with longitude increasing first. For each period $i$ the predicted number of gamma-ray events in subcell $j$ based on the total observations is :

$$n_{ij} = f_i\, e_{ij} \frac{\sum_k \left(n^0_{kj} - f_k\, e_{kj}\, \Delta I_{\mathrm{B}k}\right)}{\sum_k f_k\, e_{kj}} + f_i\, e_{ij}\, \Delta I_{\mathrm{B}i}\,, \quad (1)$$

where the sum is over all periods in which the subcell was observed and :

$n^0_{kj}$ = number of events observed in subcell $j$ in period $k$ ;

$f_i$ = sensitivity relative to the first period $(i = 0)$,

$e_{ij}$ = nominal exposure (in cm$^2$ sr s) to subcell $j$ in period $i$ (uncorrected for temporal variations), $\Delta I_{\mathrm{B}i}$ = change in background in period $i$ relative to period 0.

We define :

$$\chi^2 = \sum_i \sum_m \frac{r^2_{im}}{N_{im}}\,, \quad (2)$$

where

$$N_{im} = \sum_{j \subset \text{cell } m} n_{ij}, \qquad r_{im} = N^0_{im} - \acute{N}_{im}\,,$$

with

$$N^0_{im} = \sum_{j \subset \text{cell } m} n^0_{ij}\,.$$

The background variation was found from independent studies to correlate with the solar-modulated cosmic ray intensity. This confirmed the expectation that the background is mainly due to $\gamma$-rays produced by cosmic-ray interactions with the material in front of the telescope. On this basis the *background variation* was assumed to

have the form $\Delta I_{Bi} = b\,\Delta S_3$ where $\Delta S_3$ is the change in rate of the scaler $S_3$. The constant $b$ was determined in the analysis along with the sensitivities.

In order to avoid any correlation of sensitivity with position on the sky (see Sect. 1), a *fluctuation parameter* $S$ is defined by :

$$S = \sum_i \left(1 - \frac{f_i}{\hat{f}_i}\right)^2 , \qquad (3)$$

where $\hat{f}_i$ is chosen to fit the temporal smooth long-term trend as follows :

$$\hat{f}_i = f_A \qquad i < 30$$

$$= f_A\,(1 - a\,(i - 30)\,) \qquad i > 30 , \qquad (4)$$

where $f_A$ and $a$ are determined directly from the $f_i$. The function $\hat{f}_i$ gives a parametrized form of the long-term trend, and is based on the fact that no systematic trend is seen up to period 30, whereafter a slow decrease, consistent with a linear function of $i$, is evident.

FITTING PROCEDURE. — We require to minimize $\chi^2$ subject to the constraint of fixed $S$. To do this we minimize the quantity :

$$Y = \chi^2 + \lambda S . \qquad (5)$$

The quantity $\lambda$ acts as a Lagrangian multiplier which ensures that $\chi^2$ is minimized on $S$ = constant. The value of $\lambda$ appropriate to a given $S$ is determined empirically.

The minimization was done over the $f_i$ and $b$. Since all the sensitivities are relative to period 0 by convention, $f_0 = 1.0$.

The strategy actually followed in each energy range was as follows :

(1) using a trial value of $\lambda$, minimize $Y$ to obtain a first estimate of $b$ ;

(2) using this $b$, minimize $Y$ for various $\lambda$ ; hence obtain $S\,(\lambda\,)$ ;

(3) interpolate to find $\lambda\,(S_0)$ where $S_0$ is the selected value of $S$ ;

(4) using this $\lambda$ minimize $Y$ to find the final values the $f_i$ and $b$.

This procedure was carried out for the total energy range 70-5000 MeV and for the separate ranges 70-150, 150-300 and 300-5000 MeV ; in this way independent determinations of the parameters were obtained for estimation of the errors involved and to check for energy-dependent effects.

The range 70-5000 MeV was used as a standard in the determination of the $f_i$ because it has the highest statistical weight and, as will be shown, because there is no evidence for a significant energy dependence in the variation of sensitivity. Having determined $f_i\,(70 - 5000)$, these values could be used as input to determine the background variation parameter $b$ in each of the separate energy ranges, by minimizing $\chi^2$. This ensures consistency between the finally adopted $f_i$ and the $b$ values.

A NOTE ON THE MINIMIZATION PROBLEM. — This is a non-trivial problem because of the large number (55) of variables involved and the considerable computational requirements involved in the $\chi^2$ statistic (which uses about 750 residuals). Conjugate gradient routines in the Numerical Algorithms Group (NAG) library using only $\chi^2$ and its first derivatives were not able to find a minimum within a reasonable number of function evaluations ; however a NAG routine (E04GCF : single precision implementation) which is specially adapted to functions which are sums of squares and for which the first derivative of each term in the sum is available, was found to be very efficient at finding the minimum. About 13 function evaluations were sufficient.

## 4. Results.

The technique was applied to 55 observation periods with pointing directions $|\,b\,| < 31°$, this limit being chosen to ensure sufficient overlap with other periods for the field of view of radius 20°. Figure 1 shows the distribution of pointing directions for the periods used. The exposure values $e_{ij}$ were calculated using accelerator calibration data and assuming an $E^{-2}$ input spectrum, a sufficiently good approximation for the present purpose.

Figure 2 shows the variation of $\chi^2$ with $S$ at minimum $Y$ (Eq. (5)) obtained by varying $\lambda$, for the total energy range 70-5000 MeV. The background parameter $b$ used here is that found in the final fitting. The value of $\chi^2$ increases rapidly below $S = 0.6$ indicating that lower $S$ values are not acceptable. This value of $S$ corresponds to an r.m.s. fluctuation about the trend of 11 % ; since the fluctuations between individual periods are known to be of this order (from studies of particular overlapping regions) the value $S_0 = 0.6$ was adopted as the standard constraint in the following fits.

The change in $\chi^2$ from its large-$S$ limit to its value at $S = 0.6$ $(\lambda = 23)$ corresponds to a probability of roughly 1 %. The case $S = 0.37$ $(\lambda = 35)$ clearly corresponds to an extreme bias towards a smooth variation of the $f_i$.

Using $\lambda$ values appropriate to $S = 0.6$ the variation of $\chi^2$ with $b$ was determined for the total energy range and each separate range by minimizing $Y$ (Fig. 3 (a, b)). For each range the minimum $\chi^2$ value of $b$ is positive, corresponding to a long-term decrease in the background with time, as expected. Figure 3 indicates that the errors on the $b$ value are rather large, since the 1 $\sigma$ level corresponds formally to a change in $\chi^2$ of about 26. However the effect of the additional freedom allowed by the $S$ parameter and its associated parameters $f_A$ and $a$ (Eq. (4)) is to widen the $\chi^2$ curve, so that the real error is actually smaller than this would indicate. A further discussion of the background variation is given in section 5.

The parameters corresponding to the minima in figure 3 are summarized in the tables. Table I(a) gives the fitted parameters for the 70-5000 MeV range, and table II and figure 4(a) give the corresponding sensitivities.

Results for the separate energy ranges are given in table I(b), and the corresponding sensitivities are plotted in figure 4(b). Table I($b_i$) gives the results when both $f_i$ and $b$ are free parameters ; table I($b_{ii}$) shows the effect of fixing the $f_i$ to the values found for 70-5000 MeV and fitting only $b$. This is the appropriate procedure under the assumption (discussed below) that the $f_i$ are energy independent.

In figure 4(b), the sensitivity values have been normalized to give the same average for periods 0-30 in each energy range, thus avoiding giving special status to period 0 in the comparison. Figure 4(b) does give a slight indication for less sensitivity decrease in the low energy range ; however the effect is small, and might be due to a systematic effect — the angular resolution in the low-energy interval is relatively poor, making it harder to separate fully the reduction in sensitivity and background level. Therefore we choose to adopt the assumption of $f_i$ energy-independent. Since the three ranges are statistically independent the scatter in figure 4(b) gives an indication of the statistical error associated with each $f_i$ value. From figure 4(b) we conclude that the statistical error on $f_i$ is never more than 10 % and is generally about 5 %.

In order to illustrate the effect of the fluctuation parameter constraint, figure 5 shows $f_i$ (70-5000 MeV) for various values of $S$. The degree to which the parameters are determined by overlapping periods can be judged by the variation with $S$: well-determined values are quite insensitive to $S$, while poorly-determined values change appreciably. As mentioned above the case $\lambda = 35$ ($S = 0.37$) corresponds to an extreme lower limit on the possible fluctuations in sensitivity.

It is important to check that the method is not subject to problems arising from the lack of information on the relative sensitivity for periods with pointing directions far apart on the sky. The use of the $S$ parameter is designed to prevent this. Figure 6 shows the sensitivity values of figure 4(a) as a function of the longitude of the corresponding pointing direction ; the absence of any trend with longitude demonstrates that the method is very successful in this respect.

Since it is foreseen that some analyses will require the use of energy ranges different from the ones used here, we have determined the values of $b$ for the ranges 50-100, 100-200, 200-400, 400-800 and 800-9999 MeV, assuming the $f_i$ values given in table II(a). The $b$ values for all ranges are summarized in table I(c).

## 5. Discussion and related results.

5.1 SENSITIVITY VARIATIONS. — We have shown that the variation of instrumental sensitivity and background can be successfully derived using only the information contained in the multiple observations of the galactic plane. We see that, apart from the long-term trends, there are short-term fluctuations in sensitivity which are certainly real and not related to defects in the present method. The larger variations can be understood in terms of known changes in instrumental configuration or malfunctions in the spark-chamber, and this gives an essential check on the reliability of the present method. The origin of some of the more important deviations from the long-term trend will now be discussed.

In the earlier part of the mission, periods 8, 12 and 19 appear as having particularly low sensitivity. The origin of this effect is the delayed triggering of the charging of the odd numbered sparkchamber planes, and has been described in detail for periods around 12 by Hermsen (1980). The problem was cured by a « burn-in » procedure consisting of frequent triggering with increased high voltage, in this case during period 13, and the effect is shown clearly in the present analysis.

An independent indication of variations in sensitivity is given by the rate of $\gamma$-ray detections within a period ; strong fluctuations indicate instrumental malfunctions and the effective average sensitivity can be estimated, assuming the efficiency to be « normal » when the rate is at its maximum. Rate plots confirm the low efficiency in periods 8, 12, 19 and 56.

The good correlation of the results of the present analysis with the known instrumental effects gives confidence in the reliability of the method, which includes in addition any other sources of variation such as the manual editing of events and long-term degradation of the experiment.

5.2 BACKGROUND VARIATION FROM HIGH-LATITUDE OBSERVATIONS. — Six out of the 65 observation periods were directed towards very high latitudes ($| b | > 65°$, see Tab. III). For these periods the diffuse galactic emission is weak and the observed intensity is dominated by the instrumental background, so that these observations give an indication of the temporal variation of this background. Since there is no independent method to determine the sensitivity for these periods (they do not overlap with the lower-latitude periods and so were not included in the main analysis of this paper) it has been estimated by interpolation in figure 4(a). The values used are indicated by an asterisk in table II.

Figure 7 shows the 70-5000 MeV intensity for these periods averaged over the field of view of 20° radius, together with the predicted variation based on the $S_3$ rates as described in the previous sections. The error bars shown correspond to an estimated uncertainty of 10 % in the $f_i$ values for these periods. The absolute level of the $S_3$ predictions has been adjusted to give the same mean level as the observations. The high-latitude periods confirm the decrease in background found in the overlap analysis, and may in fact indicate a larger variation. Since a small error in the sensitivities assumed for these periods has a large effect on the derived intensities, there is no serious inconsistency.

The spectrum of the background variation (i.e. of $b$) can be compared with the spectrum of absolute intensities

at high-latitudes. The latter have spectral ratios (normalized to 1.0) of 0.53 : 0.25 : 0.22 (70-150 : 150-300 : 300-5000 MeV), while the corresponding ratios for $b$ are 0.53 : 0.19 : 0.29 for the fits with $f_i$ free (Tab. I($b_i$)) and 0.35 : 0.32 : 0.33 for the fit constrained to a common $f_i$ (Tab. I($b_{ii}$)). The more satisfactory agreement when $f_i$ is free may reflect the existence of a small energy dependence of the sensitivities ; on the other hand since the total background includes other components (extra-galactic and residual galactic emission) there is no reason to expect precise agreement between the spectra of the background variation and the total background.

A more precise evaluation of the background variation may be possible using more periods at lower latitudes, together with models for the galactic emission. This is beyond the scope of the present paper, but will be the subject of future work.

5.3 RECOMMENDED PARAMETERS FOR USE OF DATABASE. — It has been shown that the temporal dependence of the instrumental parameters can be determined with reasonable precision, but that uncertainties remain. In general the best procedure when constructing intensity maps from the data is to use the sensitivity values given in table II(a) together with the background parameters in table I($b_{ii}$). This gives the best parameters under the assumption (shown in Sect. 4 to be reasonable) that the sensitivity variation is energy-independent. For critical scientific analysis however, the effect of the uncertainties should be considered, and this can be done by varying the adopted sensitivities within the range indicated by figure 4(b), and by considering the effect of an increase in the background parameter $b(E)$ by up to a factor 2 from the recommended values. Note that this range implies a background variation which is in the range 25-50 % of the total background note also that the changes in sensitivity and background are anti-correlated.

Alternative choice of background parameters could also be made : for example if it were to be assumed that the spectrum of the background variation is in fact the same as that of the high-latitude intensity, then the $b$ values would be obtained from $b$ (70-5000 Mev) using the high-latitude spectral ratios given in section 5. For most applications the effect of these changes will be small, but they allow a good indication of the effect of systematic uncertainties on the analysis.

## 6. Inclination dependence of instrumental background.

Since the instrumental background is due to $\gamma$-rays produced in the detector, its intensity (as defined in terms of the standard sensitive area calculations) is not necessarily constant as a function of inclination from the detector axis. The actual variation of background intensity with inclination can be studied using high-latitude pointings, where the celestial emission is significantly less than the instrumental background.

For this study we have used data for $|b| > 30°$ and observation periods with pointing directions $|b_p| > 20°$. Three of these observation periods include the quasar 3C273 in the field ; for these a region of 5° radius around this source was excluded. Table III summarizes the parameters of the periods used. In order to test for deviations from a flat background, the intensity as a function of inclination averaged over all the periods used was computed using the standard sensitive areas for an $E^{-2}$ input spectrum (Fig. 8). Three standard energy ranges 70-150, 150-300 and 300-5000 MeV were used. For other reasonable input spectra the results are very similar.

Although at high energies the distribution is consistent with a flat background, at low energies a falloff with inclination is evident. This complicating feature of the COS-B data means that it is necessary in principle to determine the inclination dependence of the background for each energy range used ; however a simpler solution has been found. Figure 9 shows the *rate* of events (units photons $sr^{-1} s^{-1}$), normalized to the same total counts, as a function of inclination for the usual three energy ranges ; this rate is seen to have the *same dependence* in each range within the statistical errors. This effect, although not foreseen on the basis of knowledge of the experiment, leads to the following formula to describe the background counts in any energy range :

$$n_B = I_B(\theta = 0, t)\, A(\theta = 0)\, F(\theta)\, \Omega f t\,, \quad (6)$$

where $I_B(0, t)$ is the background intensity on-axis ($\theta = 0$) at time $t$, $A(\theta)$ is the sensitive area at inclination $\theta$, $F(\theta)$ is the rate relative to $\theta = 0$, $f$ is the relative sensitivity for the period, $\Omega$ is the solid angle of the bin and $t$ is the useful time. The form of $F(\theta)$ can be fitted by the function :

$$F(\theta) = 1 + a_1\theta + a_2\theta^2\,, \quad (7)$$

where $a_1$ and $a_2$ are constants determined by a least-squares fit to the total 70-5000 MeV energy range. Table IV summarizes the values found for both $|b| > 30°$ and $|b| > 40°$; the difference is small indicating that the effect of galactic emission on the result is not important. Figure 10 shows the data and fit for 70-5000 MeV.

RELATION TO « AVERAGE » BACKGROUND. — It is often useful to relate the value of $I_B(0, t)$ defined above to the average background over the field of view, $\hat{I}_B(t)$. A convenient definition of $\hat{I}_B(t)$ is obtained *via* the relation :

$$\hat{I}_B(t) \int_0^{\theta_{max}} A(\theta)\, d\Omega = I_B(0, t)\, A(0) \times \times \int_0^{\theta_{max}} F(\theta)\, d\Omega\,, \quad (8)$$

i.e. the flat background which gives the same total background counts over the field of view. It is convenient to define $K = \hat{I}_B(t) / I_B(0, t)$ ; values of $K$ for various energy ranges for $\theta_{max} = 20°$ are given in table V.

**7. General formulae for sensitivity and background corrections.**

Since both time dependent (described in Sect. 4) and inclination dependent (Sect. 6) variations in the response are present, it is necessary to make the appropriate corrections in astrophysical analyses related to diffuse emission. A common application is fitting to a function of the form :

$$I_{\gamma,\,\mathrm{pred}} = I_\gamma + I_{\mathrm{iso}}\,, \tag{9}$$

where $I_\gamma$ is the galactic intensity (as predicted from a model) and $I_{\mathrm{iso}}$ is a general isotropic term, containing cosmic emission not accounted for by the model and also the instrumental background.

In order to use such a formulation in the presence of the background variations we use the formula for the time dependence of $I_B$ from section 3 to give the expected background in period $i$ :

$$\hat{I}_B(i) = \hat{I}_B(i=0) + b\,\Delta S_3\,. \tag{10}$$

The expected counts in an infinitesimal bin at inclination $\theta$ in period $i$ can then be written :

$$n_i = \Omega f_i t_i \left\{A(\theta)\, I_\gamma + A(0) \times \right. \\ \left. \times \left(I_B^0 + \frac{b}{K}\Delta S_3(i)\right) F(\theta)\right\}, \tag{11}$$

where $I_B^0 = I_B(\theta = 0, i = 0)$. Defining a correction term :

$$\Delta n_B(i) = \Omega f_i t_i \left\{\left(I_B^0 + \frac{b}{K}\Delta S_3(i)\right) \times \right. \\ \left. \times F(\theta)\, A(0) - I_B^0 A(\theta)\right\}, \tag{12}$$

and writing the predicted counts including background variations :

$$n_i = \Omega f_i t_i A(\theta)\left(I_\gamma + I_B^0\right) + \Delta n_B(i)\,, \tag{13}$$

we have a relation of the required form (9) with $I_{\mathrm{iso}} = I_B^0$. $\Delta n_B$ is the correction to the predicted counts necessary to account for the two forms of background variation. It is finally possible to define the predicted total counts for all relevant observation periods :

$$\sum_i n_i = \left(I_\gamma + I_B^0\right) \sum_i \Omega f_i t_i A(\theta) + \sum_i \Delta n_B(i)\,, \tag{14}$$

which can be directly compared with the total number of counts actually observed.

The value of $I_B^0$ is not known *a priori* for insertion in the correction term (12), but it can be derived for example from fits to models of high-latitude galactic emission. At present the best values are from the intermediate-latitude study by Strong *et al.* (1985). Note however that the choice of $I_B^0$ is not critical since it only appears as a second-order term in equation (12). Values of $I_B^0$ are given in table V.

EXAMPLE OF FITTING APPLICATION. — In order to clarify the above description we give an example of the use of the data to fit an astrophysical model, in which gas column densities (convolved with the instrument point-spread function) $N_H$ are used to predict the intensity *via* :

$$I_\gamma = \frac{q}{4\pi} N_H + I_{\mathrm{iso}}\,, \tag{15}$$

where $q$ is the $\gamma$-ray emissivity. The appropriate likelihood function is then :

$$L\left(q, I_{\mathrm{iso}}\right) = \prod_{\mathrm{skybins}} \frac{\mathrm{e}^{-x} x^\mu}{\mu!}, \tag{16}$$

where $x = \sum n_i$, $\mu = \sum n_{0,i}$, where $n_i$ is given by equation (13), $n_{0,i}$ is the observed count in a skybin in one period, and the sum is over observation periods. If the model is satisfactory then $I_{\mathrm{iso}}$ from the fit should be close to $I_B^0$, and this is sufficient to ensure consistency with the definition of $\Delta n_B$.

DERIVATION OF CORRECTED GAMMA-RAY INTENSITY. — For many applications it is necessary to use the data directly to give an intensity. This must be corrected for the background variations ; a suitable definition is :

$$I_{\gamma,\,\mathrm{corr}} = \frac{\sum_i \left(n_i - \Delta n_B(i)\right)}{\sum_i A(\theta)\,\Omega f_i t_i}, \tag{17}$$

which is standardized to the on-axis background at Period 0. This is the recommended « intensity » when using COS-B data. Note that usually $\Delta n_B$ is negative since the background generally decreases both with time and inclination.

SOFTWARE IMPLEMENTATION. — The definition of $\Delta n_B$ is that used for the background correction term in the FADMAP program included with the COS-B database as standard software for skymap production. The quantities $\sum n_0$, $\sum Aft$ and $\sum \Delta n_b$ are given in the FITS skymap datasets included in the database (see the Explanatory Supplement, Mayer-Hasselwander, 1985).

**Acknowledgements.**

The Laboratory for Space Research Leiden is supported financially by ZWO, the Netherlands Organization for the Advancement of Pure Research.

## References

HERMSEN, W. : 1980, Thesis, University of Leiden.
MAYER-HASSELWANDER, H. A. : 1985, *Explanatory Supplement to the COS-B Final Database,* obtainable from K. Bennett, Space Science Department of ESA, ESTEC (Noordwijk, The Netherlands).
MAYER-HASSELWANDER, H. A., *et al.* : 1986, in preparation.
STRONG, A. W., BLOEMEN, J. B. G. M., HERMSEN, W., MAYER-HASSELWANDER, H. A. : 1985, *Proc. XIX Int. Cosmic Ray Conf.* **1,** 317.

TABLE I. — *Background and trend parameters derived from fitting.*

Maximum absolute latitude of pointing = 30.2°
Number of periods included = 55
Number of 100 sq. deg. cells = 748

(a) Total energy range

| Energy | $\lambda$ | S | $f_A$ | $a$ | $b$ | $\chi^2$ |
|---|---|---|---|---|---|---|
| 70-5000 | 23 | 0.615 | 0.957 | 0.0146 | $1.9\ 10^{-6}$ | 954.5 |

(b) Three separate energy ranges
(i) Fit free in all variables

| Energy | $\lambda$ | S | $f_A$ | $a$ | $b$ | $\chi^2$ |
|---|---|---|---|---|---|---|
| 70- 150 | 17 | 0.606 | 0.965 | 0.0312 | $1.25\ 10^{-6}$ | 743.6 |
| 150- 300 | 12 | 0.629 | 0.922 | 0.0513 | $0.45\ 10^{-6}$ | 629.2 |
| 300-5000 | 15 | 0.611 | 0.921 | 0.0145 | $0.68\ 10^{-6}$ | 713.8 |

(ii) Fit to background parameter b based on sensitivities for 70-5000 MeV.

| Energy | b |
|---|---|
| 70-150 | $0.73\ 10^{-6}$ |
| 150-300 | $0.67\ 10^{-6}$ |
| 300-5000 | $0.69\ 10^{-6}$ |

(c) Background parameter b for additional energy ranges, based on sensitivities for 70-5000 MeV

| Energy | b |
|---|---|
| 50-100 MeV | $1.8\ 10^{-6}$ |
| 100-200 | $0.29\ 10^{-6}$ |
| 200-400 | $0.51\ 10^{-6}$ |
| 400-800 | $0.21\ 10^{-6}$ |
| 800-5000 | $0.39\ 10^{-6}$ |

TABLE II(a). — *Sensitivity values for the energy interval 70-5000 MeV.*

Maximum absolute pointing latitude = 30.2°
Number of periods included = 55
Number of 100 sq. degree cells = 748
*Periods marked with an asterisk had insufficient overlap to be included in the fitting scheme; the values given are obtained by interpolation between the preceding and succeeding periods.*

| Period | f | Period | f |
|---|---|---|---|
| 0 | 1.00 | | |
| 1 | 0.95 | 31 | 0.99* |
| 2 | 1.02 | 32 | 0.99* |
| 3 | 1.03 | 33 | 0.98 |
| 4 | 0.92 | 34 | 1.00 |
| 5 | 0.93 | 35 | 0.94 |
| 6 | 0.89 | 36 | 0.93 |
| 7 | 1.03 | 37 | 0.89 |
| 8 | 0.78 | 38 | 0.78 |
| 9 | 0.98 | 39 | 0.69 |
| 10 | 0.93* | 40 | 0.84 |
| 11 | 0.88 | 41 | 0.78* |
| 12 | 0.78 | 42 | 0.72 |
| 13 | 0.91 | 43 | 0.84 |
| 14 | 0.97 | 44 | 0.66 |
| 15 | 0.99* | 45 | 0.73 |
| 16 | 1.00 | 46 | 0.74* |
| 17 | 1.05 | 47 | 0.75 |
| 18 | 1.00 | 48 | 0.64 |
| 19 | 0.79 | 49 | 0.69 |
| 20 | 1.04 | 50 | 0.66 |
| 21 | 1.00 | 51 | 0.68 |
| 22 | 0.96 | 52 | 0.65* |
| 23 | 0.98* | 53 | 0.62 |
| 24 | 1.01 | 54 | 0.47 |
| 25 | 0.97 | 55 | 0.53 |
| 26 | 1.00 | 56 | 0.37 |
| 27 | 0.99* | 57 | 0.59 |
| 28 | 0.98 | 58 | 0.68 |
| 29 | 1.02 | 59 | 0.53 |
| 30 | 1.00 | 60 | 0.53 |
| | | 61 | 0.43 |
| | | 62 | 0.47 |
| | | 63 | 0.56 |
| | | 64 | 0.55 |

TABLE III. — *Observation periods used in background study.*

| Period Number | Pointing Direction Longitude | Latitude |
|---|---|---|
| 10 | 283.5 | 68.6 |
| 15 | 301.0 | -43.7 |
| 23 | 300.0 | 44.8 |
| 27 | 154.6 | 82.7 |
| 30 | 358.6 | -30.2 |
| 31 | 228.2 | 44.1 |
| 32 | 289.6 | 64.4 |
| 35 | 111.6 | 27.2 |
| 37 | 118.1 | -20.1 |
| 41 | 45.2 | -61.4 |
| 43 | 190.6 | -26.8 |
| 46 | 183.2 | 64.7 |
| 48 | 355.5 | 20.0 |
| 50 | 6.5 | -27.7 |
| 52 | 300.5 | 65.6 |
| 53 | 16.0 | 25.5 |

TABLE IV. — *Results of fits to equation (7).*

Latitude range of observation pointings: $|b| > 20°$

| Energy range MeV | $\lvert b\rvert > 30°$ $a_1$ $10^{-2}$ | $a_2$ $10^{-4}$ | $\lvert b\rvert > 40°$ $a_1$ $10^{-2}$ | $a_2$ $10^{-4}$ |
|---|---|---|---|---|
| 70- 150 | -5.64 | 8.50 | -5.98 | 9.98 |
| 150- 300 | -5.52 | 8.17 | -4.98 | 5.95 |
| 300-5000 | -5.72 | 9.00 | -5.40 | 7.90 |
| 70-5000 | -5.63 | 8.55 | -5.55 | 8.33 |

TABLE V. — *Values of* $I_B^0$ *and* $K\left(=\hat{I}_B/I_B^0\right)$ *for various energy ranges.*

Inclination range over which averages are defined: $0 < \theta < 20°$

| Energy range MeV | $I_B^0$ $10^{-5} cm^{-2} sr^{-1} s^{-1}$ | $K$ |
|---|---|---|
| 70- 150 | 7.2 | 0.659 |
| 150- 300 | 2.5 | 0.799 |
| 300-5000 | 2.2 | 0.876 |

The following values were derived by interpolation from the previous energy ranges, assuming an $E^{-2}$ dependence within each range.

| | | |
|---|---|---|
| 50-100 | 9.45 | 0.659 |
| 100-200 | 4.40 | 0.709 |
| 200-400 | 1.84 | 0.836 |
| 400-800 | 0.88 | 0.865 |
| 800-5000 | 0.74 | 0.928 |

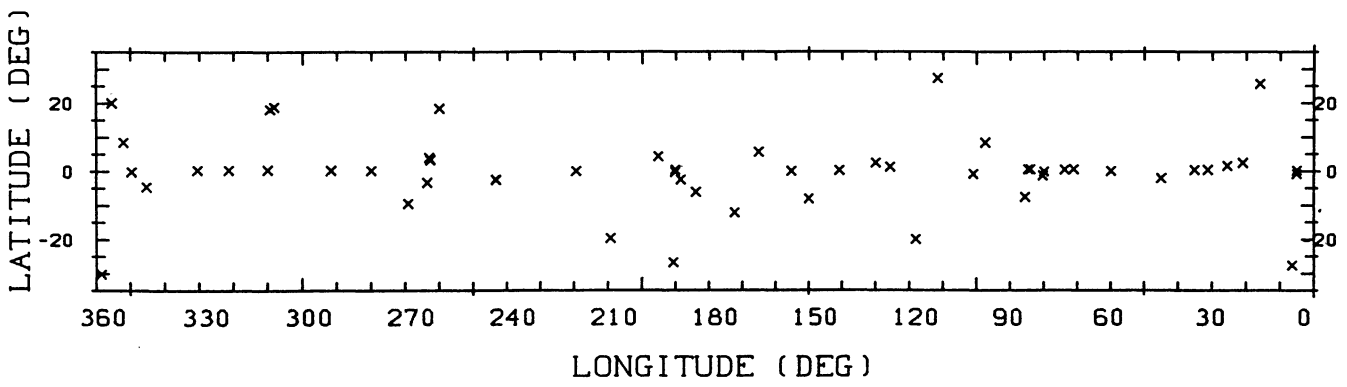


FIGURE 1. — The pointing directions of the 55 observation periods used in the multivariate optimization analysis for the determination of temporal variations in the instrument sensitivity and background level. The field of view used is a circle of radius 20° around each pointing.

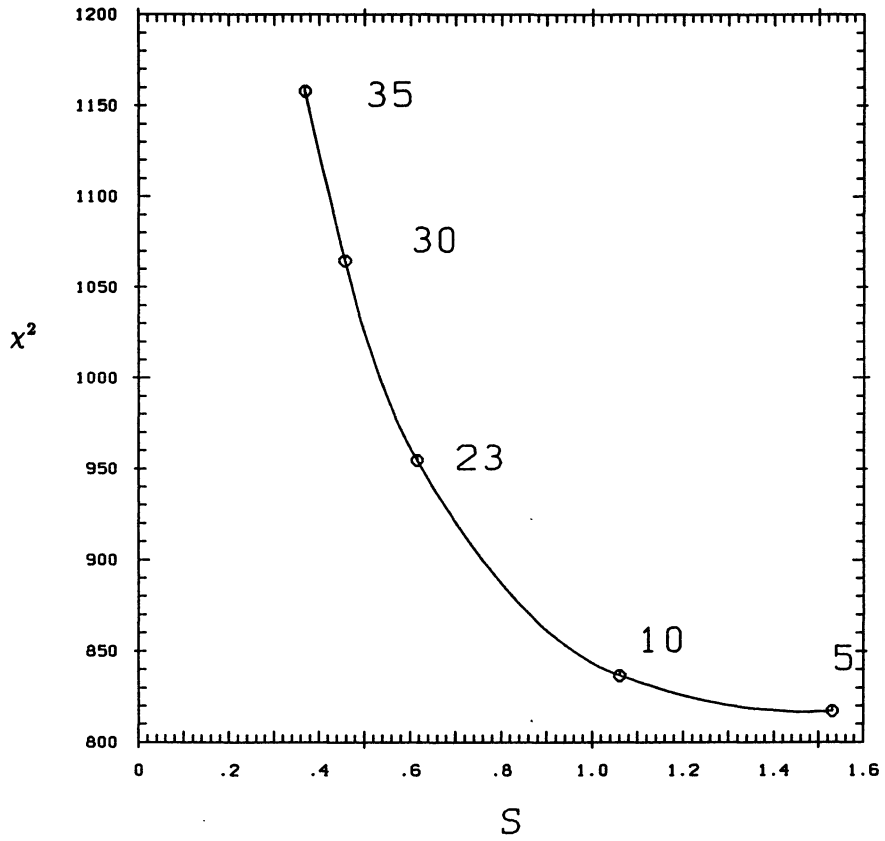


FIGURE 2. — The value of $\chi^2$ as a function of the fluctuation parameter $S$ for the energy range 70-5000 MeV. The values of the Lagrangian multiplier $\lambda$ associated with various $S$ values are also given.

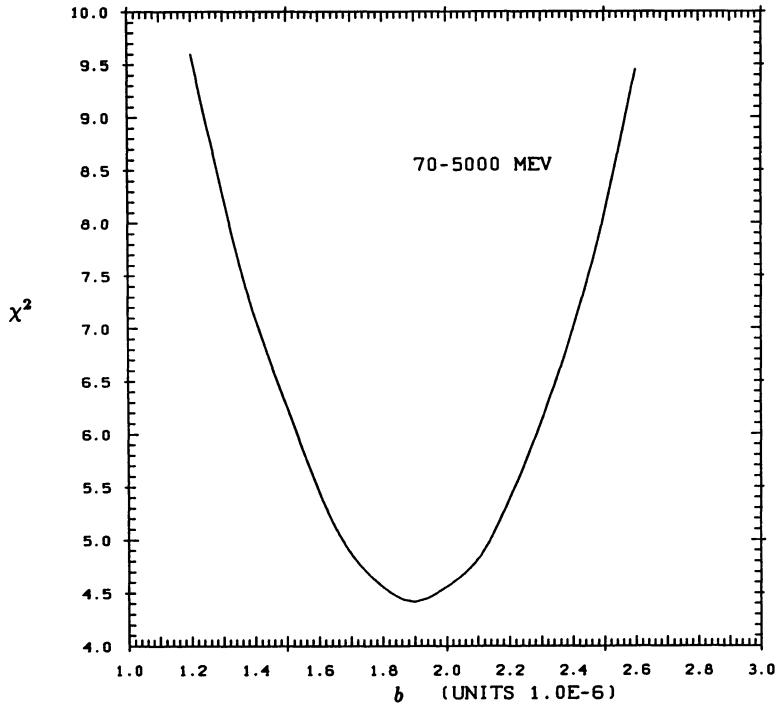


(a)

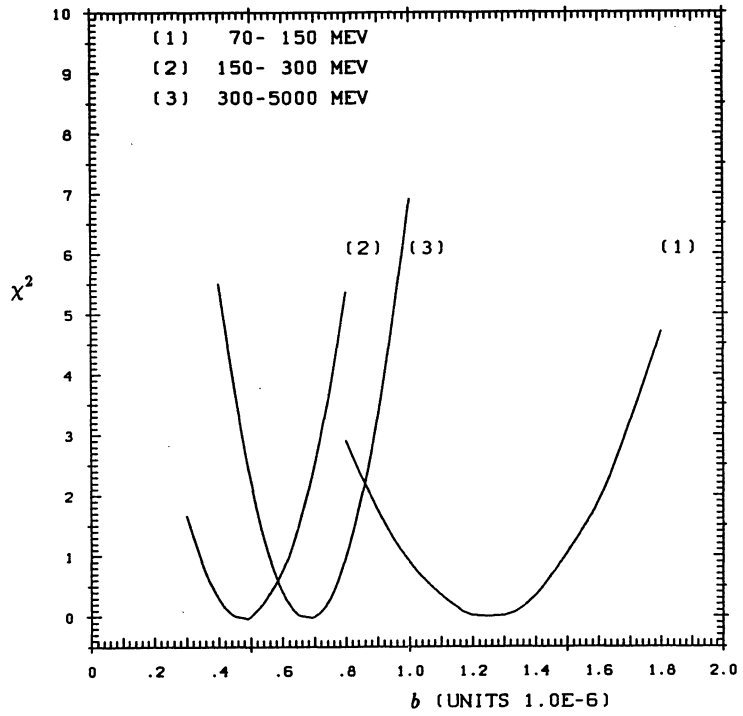


(b)

FIGURE 3. — Determination of the optimum background variation parameter $b$ for each energy range independently. $\chi^2$ minimized over the $f_i$ is shown as a function of $b$, using the values of $\lambda$ which constrain $S$ to a value near 0.6. A value near the minimum value of $\chi^2$ has been subtracted in each case ; the minima are given in tables I(a) and I($b_i$). (a) 70-5000 MeV. (b) 70-150, 150-300 and 300-5000 MeV.

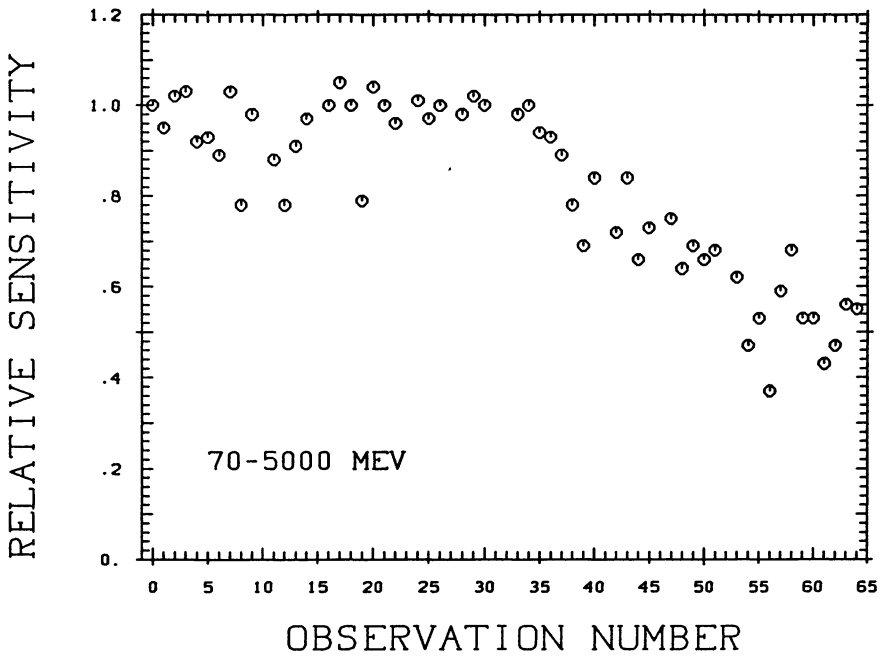


(a)

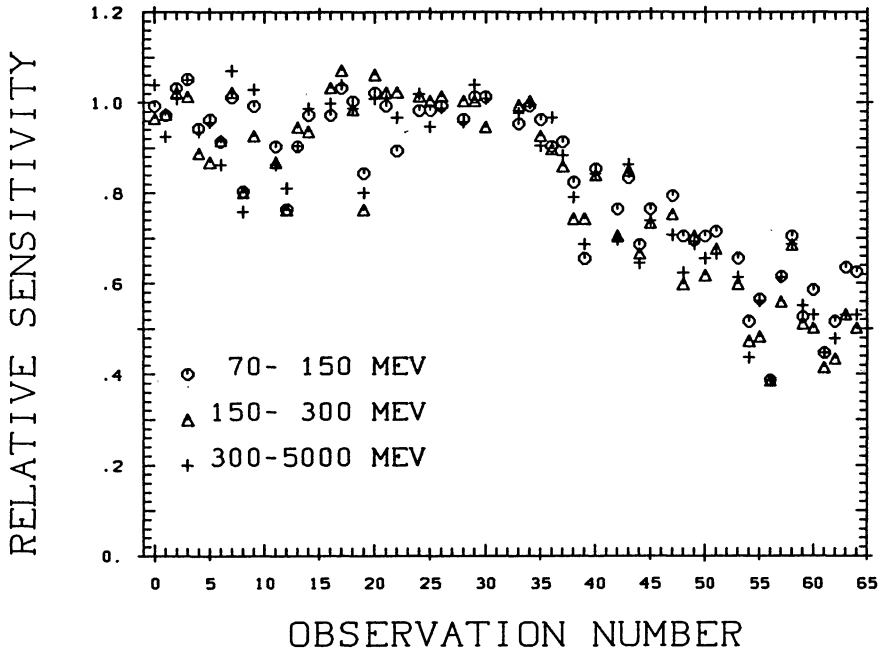


(b)

FIGURE 4. — Relative sensitivity $f_i$ for each observation period determined from the optimization algorithm. (a) 70-5000 MeV, using parameters given in table I (a). (b) 70-150 MeV (circles), 150-300 MeV (triangles), 300-5000 MeV (crosses), using the parameters given in table I($b_i$).

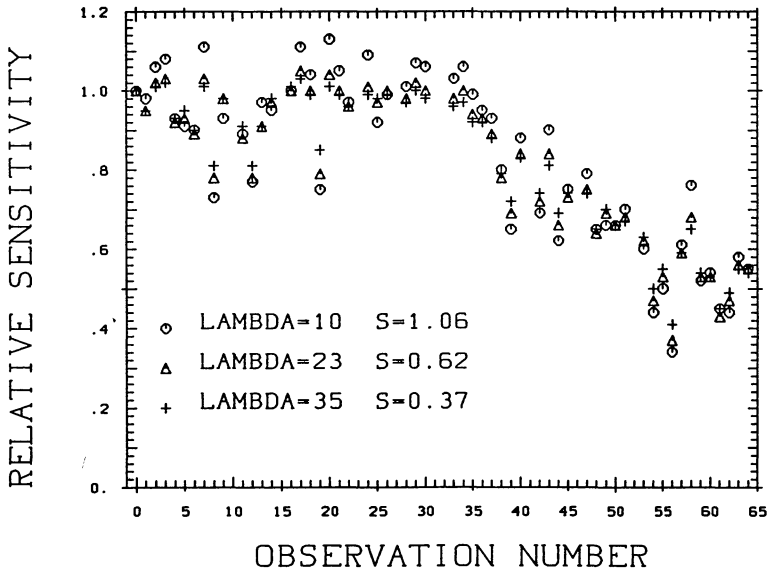


FIGURE 5. — Effect of the fluctuation parameter $S$ on the solution for the sensitivities in the 70-5000 MeV range. The solutions were obtained by varying $\lambda$ to obtain various values of $S$: $\lambda = 10$, 23, 35 giving $S = 1.06$, 0.615 and 0.368 respectively. The background parameter $b$ was fixed at $1.9 \times 10^{-6}$.

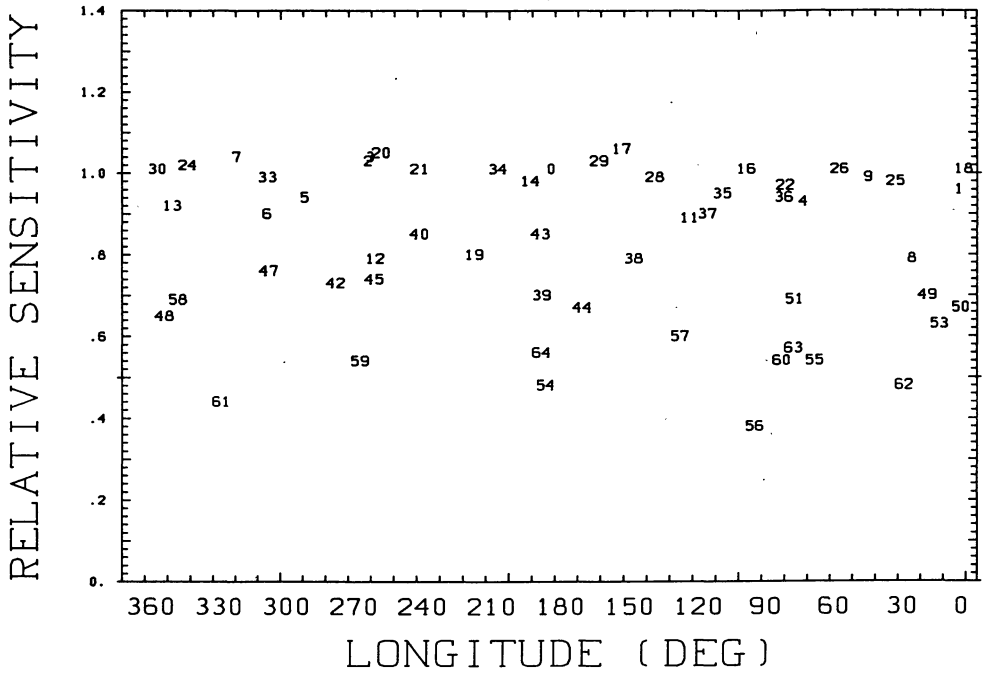


FIGURE 6. — Relative sensitivities for 70-5000 MeV as a function of the longitude of the instrument pointing direction. The numbers give the observation period index as in table II. The lack of any systematic trend shows that the method satisfactorily eliminates effects due to the lack in information to connect periods far apart on the sky.

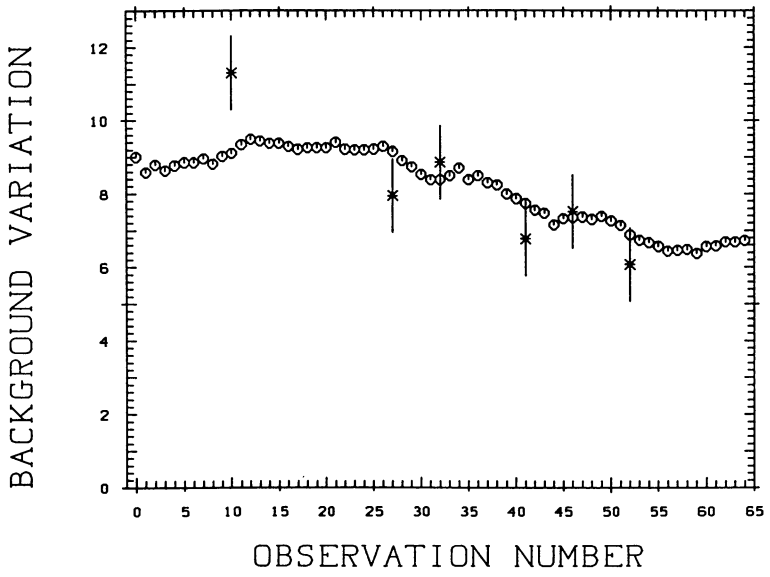


FIGURE 7. — The variation of the background for 70-5000 MeV as predicted from the $S_3$ rate, compared to the intensity in six high-latitude observations with $|b| > 65°$. Units are $10^{-5}$ cm$^{-2}$ sr$^{-1}$ s$^{-1}$. The $b$ coefficient used is $b = 2.1 \times 10^{-6}$ (circles), corresponding to the sum of the values in table I($b_{ii}$), as recommended in section 5.3. For the six high-latitude observation periods the intensity has been averaged over directions within 20° of the pointing direction, avoiding the source 3C273. The error bars reflect the estimated uncertainty of 0.1 in the relative sensitivities for the periods. Since the $S_3$ estimate gives only the *change* in background intensity, the level of the predicted values has been adjusted to give the same average value as the high-latitude observations.

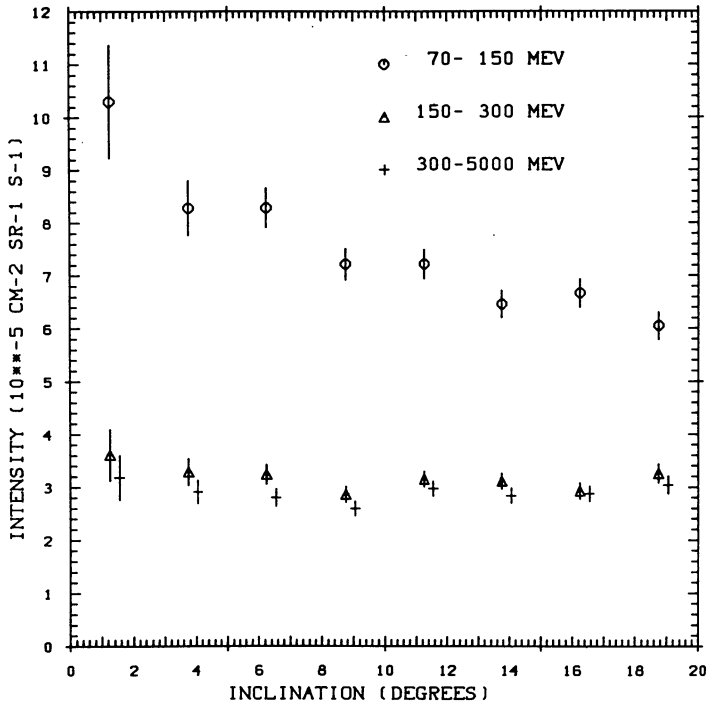


FIGURE 8. — Intensity as a function of inclination angle from the pointing axis for $|b| > 30°$, averaged over high-latitude observation periods. Error bars are statistical, $\pm 1\,\sigma$. Circles : 70-150 MeV, triangles : 150-300 MeV, crosses : 300-5000 MeV.

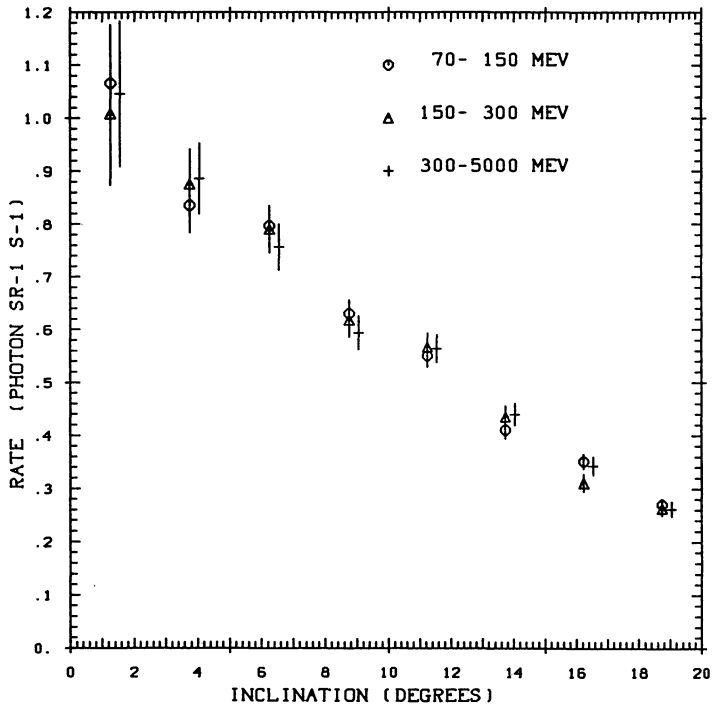


FIGURE 9. — Rate (photon $sr^{-1} s^{-1}$) as a function of inclination from the pointing axis for $| b | > 30°$, averaged over high-latitude observation periods. Error bars are statistical, $\pm 1\ \sigma$. Circles : 70-150 MeV, triangles : 150-300 MeV, crosses : 300-5000 MeV.

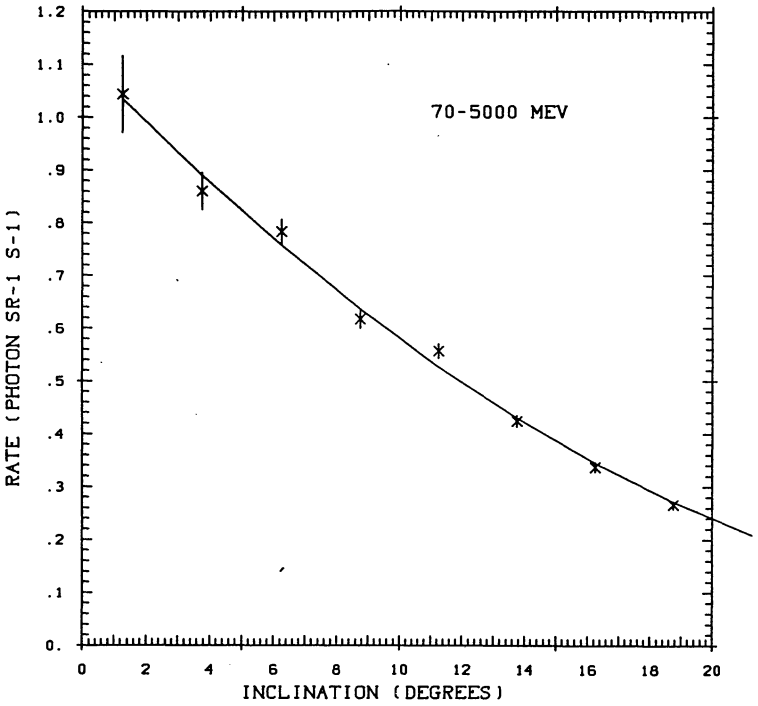


FIGURE 10. — Rate (photon $sr^{-1} s^{-1}$) as a function of inclination from the pointing axis for $| b | > 30°$, averaged over high-latitude observation periods, for 70-5000 MeV. The crosses show the data points with statistical errors, the continuous line shows the fitted expression from equation (7) with the parameters of table IV.